Supplemental Material can be found at:
http://www.jbc.org/cgi/content/full/M509486200/DC1

THE JOURNAL OF BIOLOGICAL CHEMISTRY VOL. 281, NO. 9, pp. 5364–5372, March 3, 2006
© 2006 by The American Society for Biochemistry and Molecular Biology, Inc. Printed in the U.S.A.

The Nerve Hemoglobin of the Bivalve Mollusc *Spisula solidissima*

*MOLECULAR CLONING, LIGAND BINDING STUDIES, AND PHYLOGENETIC ANALYSIS**[S]

Received for publication, August 29, 2005, and in revised form, December 7, 2005 Published, JBC Papers in Press, December 13, 2005, DOI 10.1074/jbc.M509486200

Sylvia Dewilde[‡1], Bettina Ebner[§], Evi Vinck[¶2], Kambiz Gilany[‡], Thomas Hankeln[§], Thorsten Burmester[‖], Jill Kreiling[**], Carol Reinisch[**], Jacques R. Vanfleteren[‡‡], Laurent Kiger[§§], Michael C. Marden[§§], Christian Hundahl[¶¶], Angela Fago[¶¶], Sabine Van Doorslaer[¶], and Luc Moens[‡3]

From the Departments of [‡]Biomedical Sciences and [¶]Physics, University of Antwerp, 2610 Antwerp, Belgium, [§]Institute of Molecular Genetics and [‖]Institute of Zoology, Johannes Gutenberg University, 55099 Mainz, Germany, [**]Marine Biological Laboratory, Woods Hole, Massachusetts 02543, [‡‡]Department of Biology, Ghent University, 9000 Ghent, Belgium, [§§]Inserm U779, 94276 Le Kremlin-Bicêtre, France, and [¶¶]Zoophysiology, Institute of Biological Sciences, University of Aarhus, DK-8000 Aarhus C, Denmark

Members of the hemoglobin (Hb) superfamily are present in nerve tissue of several vertebrate and invertebrate species. In vertebrates they display hexacoordinate heme iron atoms and are typically expressed at low levels (μM). Their function is still a matter of debate. In invertebrates they have a hexa- or pentacoordinate heme iron, are mostly expressed at high levels (mM), and have been suggested to have a myoglobin-like function. The native Hb of the surf clam, *Spisula solidissima*, composed of 162 amino acids, does not show specific deviations from the globin templates. UV-visible and resonance Raman spectroscopy demonstrate a hexacoordinate heme iron. Based on the sequence analogy, the histidine E7 is proposed as a sixth ligand. Kinetic and equilibrium measurements show a moderate oxygen affinity (P_{50} ~0.6 torr) and no cooperativity. The histidine binding affinity is 100-fold lower than in neuroglobin. Phylogenetic analysis demonstrates a clustering of the *S. solidissima* nerve Hb with mollusc Hbs and myoglobins, but not with the vertebrate neuroglobins. We conclude that invertebrate nerve Hbs expressed at high levels are, despite the hexacoordinate nature of their heme iron, not essentially different from other intracellular Hbs. They most likely fulfill a myoglobin-like function and enhance oxygen supply to the neurons.

The recent discovery of globin proteins in the nerve cells of mammals and other vertebrates (1) has created much interest in unraveling the cellular functions and potential biomedical implications of these oxygen binding molecules in the metabolism of the vertebrate nervous system (2). Historically, however, "nerve hemoglobins" (nHbs)[4] were first observed in invertebrate taxa. In 1872, Lankester had already recorded the brilliant red color of the ganglia of the polychaete annelid *Aphrodite aculeata* (3). Since then, nHbs have also been found in, or associated with, nerve tissues of several other invertebrate taxa, such as molluscs, arthropods, nemerteans, and nematode species (4, 5). Of these, only the nHbs of *A. aculeata* (6) and the nemertean worm *Cerebratulus lacteus* (7) have been characterized at the molecular level.

With few exceptions (*e.g.* in air-breathing gastropods), the invertebrate nHbs are expressed at high concentrations (in the mM range) and have therefore been suggested to support nerve function by mediating O_2 storage and/or transport during temporary hypoxia (4). For example, in the gastropod mollusc *Aplysia depilans*, the oxygenation state of the nHb was correlated with the electrical activity of the neural ganglia, and firing was shown to be proportional to the degree of oxygenation of the globin (8). The nHb in the nerve bundles of the bivalve mollusc *Tellina alternata* was reported to extend the time of O_2 delivery to the nerves during anoxic periods by as much as 30 min, whereas this effect was not demonstrable in the nerves of a related clam species *Tagelius plebeius*, which lack the nHb (9). In many cases, the nHbs appear to be specifically expressed in the glial cells surrounding neurons, as reported for the clams *T. alternata* and *Spisula solidissima* (10), the water-dwelling gastropods *Lymnaea stagnalis* and *Planorbis corneus* (11), the nemertean *C. lacteus* (7), and the annelid *A. aculeata* (12). In *Aplysia* and in the air-breathing gastropods *Helix pomatia* and *Cepaea nemoralis*, however, the nHbs have been detected within the neurons themselves (11, 13). The physiological implications of this cell type-specific expression are unclear.

With P_{50} values between 1.1 and 4 torr (12), the oxygen affinities of nHbs are moderate and quite similar to those of vertebrate myoglobins (Mbs), in agreement with the proposed oxygen supply function. However, spectral analyses revealed two different types of nHbs based on the coordination at the heme iron. The nHbs of *Aplysia spec.*, *A. aculeata* and *C. lacteus* are pentacoordinate, like vertebrate hemoglobins (Hbs) and Mbs, whereas those of the bivalves *T. alternata* and *S. solidissima* are hexacoordinate and exhibit a cytochrome *b*-type absorption spectrum (9, 14). In hexacoordination, an internal protein ligand (mostly the distal E7 histidine residue) occupies the sixth coordinating position of the heme iron and has to be displaced before an external gaseous ligand can be bound. This results in complex ligand binding kinetics, of which the functional implications still have to be revealed (15, 16).

Several of these features (*e.g.* hexacoordination, moderate oxygen affinity) of invertebrate nHbs are shared with the neuroglobins (Ngb), which have been identified in many vertebrate taxa, including mammals, birds, amphibians, and fishes (17). Ngb is expressed in the central

* This study was supported in part by Inserm, University of Paris-XI, by European Union Grant QLG3-CT-2002-01548, the Deutsche Forschungsgemeinschaft (Ha2103/3 and Bu956/5), by the Fund for Scientific Research of Flanders Grant G.0468.03, and by the Danish Natural Science Research Council. The costs of publication of this article were defrayed in part by the payment of page charges. This article must therefore be hereby marked "*advertisement*" in accordance with 18 U.S.C. Section 1734 solely to indicate this fact.

[S] The on-line version of this article (available at http://www.jbc.org) contains supplemental Figs. SA and SB.

[1] A postdoctoral fellow of the Fund for Scientific Research of Flanders.
[2] A research assistant of the Fund for Scientific Research of Flanders.
[3] To whom correspondence should be addressed: Dept. of Biomedical Sciences, University of Antwerp, Campus Drie eiken, Universiteitsplein 1, Antwerp B-2610, Belgium. Tel.: 32-3-8202323; Fax: 32-3-8202248; E-mail: luc.moens@ua.ac.be.

[4] The abbreviations used are: nHb, invertebrate nerve hemoglobin; Mb, myoglobin; Ngb, neuroglobin; Cygb, cytoglobin; HS, high spin; RR, resonance raman; RT, reverse transcription; P_{50}, oxygen pressure at which half saturation of the hemoglobin is obtained.

Downloaded from www.jbc.org at Marine Biological Laboratory on April 21, 2009

and peripheral nervous system, the retina, and in endocrine tissue, but it is specifically found in neurons and not in astrocytes or other glial cells (18–22). In contrast to most nHbs, Ngb is expressed at lower concentrations (μM) in the vertebrate brain, whereas it is more strongly expressed in the neuronal retina (20). Ngb also displays a *bis*-His-Fe hexacoordinate heme structure (1, 23–25). Ngb is thought to protect neurons against hypoxic damage *in vitro* and against ischemia/reperfusion injury *in vivo* (26, 27). However, its function is unclear, and several putative physiological roles of Ngb are still discussed (2).

For further understanding of both vertebrate Ngb and invertebrate nHb functions, we have aimed at the molecular characterization of the nHb of the Atlantic surf clam *S. solidissima* (14, 28, 29). This protein is an example of a hexacoordinate nHb, which is abundantly expressed in glial cells and lends the nerves of this organism a bright red appearance.

MATERIALS AND METHODS

Animals—*S. solidissima* (Mollusca, Bivalvia) were obtained from the Aquatic Resources Division, Marine Biological Laboratory, Woods Hole, MA. Nerve cords and foot and contractor muscle were dissected, frozen in liquid nitrogen, and stored at −80 °C until use.

Determination of the Partial Amino Acid Sequence of S. solidissima nHb—Nerves were thawed and homogenized in 50 mM Tris-HCl, pH 7.5, containing the Complete™ protease inhibitor mixture (Roche Diagnostics) and centrifuged 10 min at 10,000 rpm; the red supernatant was saved. The nHb was precipitated by differential ammonium sulfate precipitation at 40 and 90% saturation, respectively. Desalted samples were made up to 50 mM Tris-HCl, pH 7.5, 6 M guanidinium hydrochloride, 1% 2-mercapto-ethanol and heated for 5 min at 100 °C. Samples were acidified with 0.1% trifluoroacetic acid and separated by reversed phase chromatography on a Vydac C4 column (4.1 mm × 25 cm) using a gradient 0.1% trifluoroacetic acid, 0.5% CH_3CN to 0.1% trifluoroacetic acid, 75% CH_3CN in 45 min at a flow rate of 1 ml/min. The nHb-containing fractions were vacuum dried and digested with trypsin at an enzyme/substrate ratio of 1/50. The resulting peptides were separated on a Vydac C18 column (2.1 mm × 25 cm; flow rate, 200 μl/min) using the same gradient as for globin purification. Purified peptides were sequenced by automated Edman degradation using an ABI Prosice protein sequencer operated according to the manufacturer's instructions. Peptide sequences were aligned using the primary structure of sperm whale Mb and *A. aculeata* nHb as templates.

cDNA Library Construction—Freshly dissected nerve cords of *S. solidissima* were immediately submerged and stored in RNA*later* RNA stabilization reagent (Qiagen, Hilden, Germany) at 4 °C. RNA extraction was performed on 40 nerve cords using the RNeasy kit (Qiagen). Poly(A)$^+$ mRNA was purified from ~100 μg of total RNA according to the protocol of the Oligotex mRNA kit (Qiagen). ~0.5 μg of poly(A)$^+$ mRNA was employed for cDNA synthesis using the ZAP Express cDNA synthesis kit (Stratagene, La Jolla, CA) and Sephacryl S-500 spin columns (Stratagene) for size fractionation. The resulting double-stranded XhoI-EcoRI cDNA fractions were ligated to 1 μg of ZAP Express vector each. Packaging of the directionally cloned cDNA library was performed using the Gigapack III Gold extract (Stratagene). The resulting phage library, consisting of 10^5 clones, was amplified prior to the isolation of globin gene cDNA sequences by vector-anchored PCR (see below).

S. solidissima nHb cDNA Sequence—Degenerated primers were designed based on the partial sequence obtained at the protein level. *S. solidissima* total RNA was prepared using the TRIzol method (Invitrogen). cDNA was synthesized using random hexamer primers and Superscript RT enzyme from Invitrogen. Primer SpiF1 (5′-AARCARGAYTGGAARACN) is a 20-mer with 64-fold redundancy, corresponding to the sense strand predicted by the peptide fragment KQDWKTI. Primer SpiR1 (5′-GTYTGCATRTGNCCNCCDAT) is a 20-mer with 192-fold redundancy, corresponding to the antisense strand predicted by the peptide fragment IGGHMQ. PCR was carried out for 5 min at 94 °C (1 min at 94 °C, 1 min at 50 °C, 1 min at 72 °C) for 35 cycles and 10 min at 72 °C. The amplified product was purified and sequenced. Based on this sequence a 5′-RACE was carried out using the 5′ Rapid Amplification of cDNA Ends system for rapid amplification of cDNA ends (Invitrogen). The 3′-end of the *S. solidissima* globin cDNA was obtained from the amplified phage cDNA library by a PCR approach using the vector-specific oligonucleotide primer T3 and the gene-specific forward (5′-GATGCCGTCGCTAACAGTTG-3′) primer. Globin gene-specific primers were designed according to the partial cDNA obtained by RT-PCR and RACE. PCR amplicons were either sequenced directly or after cloning into the pGEM T-easy vector (Promega, Madison, WI) on both strands by DyeTerminator cycle sequencing chemistry (Applied Biosystems, Foster City, CA). Sequencing reactions were loaded on an Applied Biosystems Prism 3730 capillary sequencer (GENterprise, Mainz, Germany). Sequences were further analyzed using Lasergene programs (DNAstar Inc.).

Isolation and Sequencing of the S. solidissima nHb Gene Region—Genomic DNA of *S. solidissima* foot and contractor muscle of several animals was prepared by the protocol of Schmidt *et al.* (30) with minor modifications. Sets of primer pairs were designed according to the complete nHb cDNA, and overlapping genomic fragments were amplified. Sequences were obtained as described above.

Expression of the Complete Coding Sequence of the nHb of S. solidissima in Escherichia coli—Recombinant *S. solidissima* nHb were expressed as described (15). In short, the cDNA of the nHb was cloned into the expression vector pET3a. After expression in *E. coli* BL21(DE3)pLysS cells, the *S. solidissima* nHb was purified to homogeneity by using: (i) ammonium sulfate precipitation (40–90% saturation) for which the 90% pellet was dissolved and dialyzed against 5 mM Tris-HCl, pH 8.5, (ii) a DEAE-Sepharose fast flow column (step elution in 5 mM Tris-HCl, pH 8.5, 200 mM NaCl), and (iii) a Sephacryl S200 gel filtration column in 5 mM Tris-HCl, pH 8.5. The globin fractions were pooled and concentrated.

Mass Spectrometry of Native and Recombinant S. solidissima nHb—*S. solidissima* nHb in 5 mM Tris-HCl, pH 8.5, was analyzed by mass spectroscopy. The native or recombinant sample at 5 mM concentration was dissolved in 50:50 methanol:water in 5% formic acid and injected into custom-made nanoelectrospray needles. Nano-electrospray mass spectra were acquired on a Q-TOFII (Micromass, Wythwnshave, UK) over the mass-to-charge ratio (m/z) range 700–2000. The multiply charged electrospray spectra were deconvoluted by MaxEnt1 software to produce the molecular mass of the protein. Before each measurement, the mass scale was calibrated with myoglobin.

Phosphoprotein Staining—Native and recombinant *S. solidissima* nHb were analyzed by standard SDS-PAGE (15%) and native gel electrophoresis. Pro-Q Diamond phosphoprotein gel staining (Invitrogen-Molecular Probes) was performed as described by the manufacturer. As positive controls for phosphorylated proteins, ovalbumin and the peppermint marker (supplied with the staining kit) were used. Negative controls were Mb and bovine serum albumin.

Optical and Resonance Raman Spectra—Optical measurements were done with a Cary-5 UV-VIS-NIR spectrophotometer. All optical spectra were measured in a range from 350 to 700 nm. Resonance-Raman (RR) measurements were carried out on an 80-cm Dilor XY-800 Raman scattering spectrometer consisting of a triple spectrograph operating in nor-

Downloaded from www.jbc.org at Marine Biological Laboratory on April 21, 2009

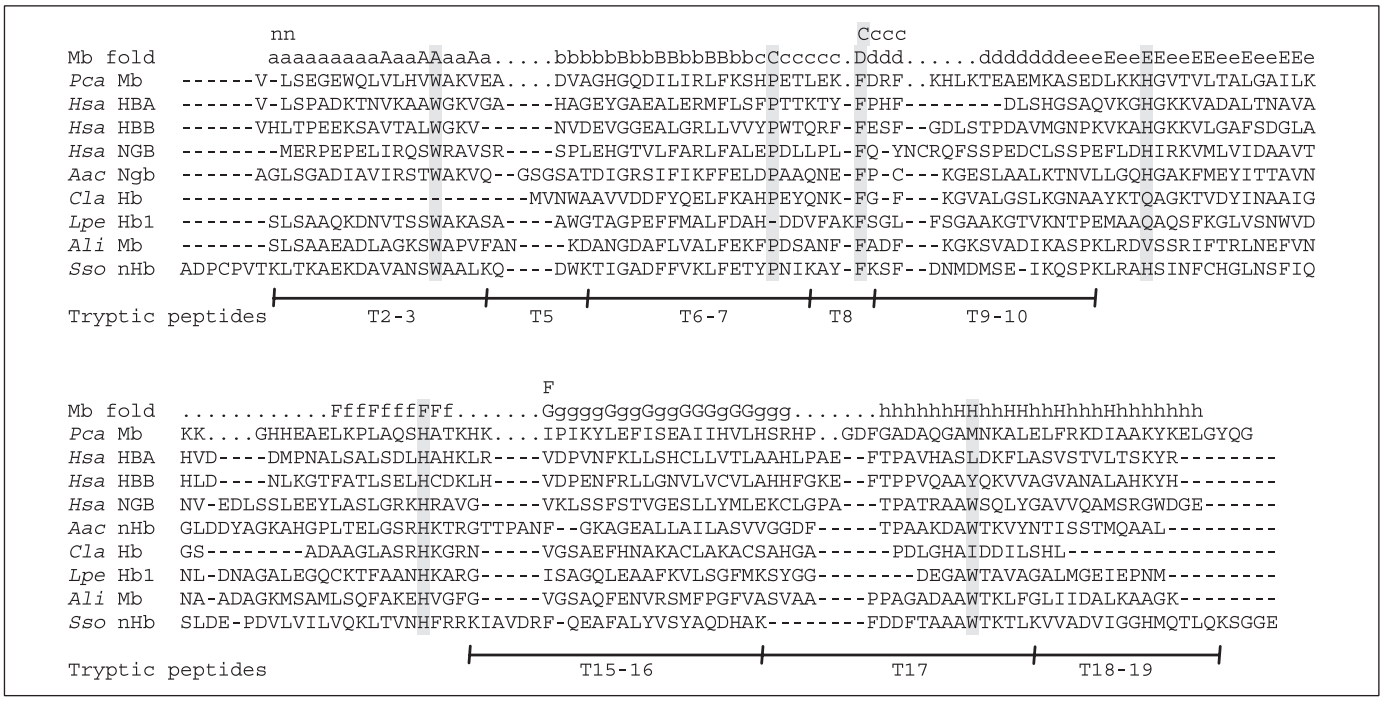

FIGURE 1. **Alignment of selected globin amino acid sequences based on the myoglobin fold.** The key topological residues (*A12*, *C2*, *CD1*, *E7*, *F8*, *H8*) are *highlighted*. Abbreviations used are *Pca Mb*, *Physeter catodon* myoglobin; *Hsa HBA*, *H. sapiens* α-chain hemoglobin; *Hsa HBB*, *H. sapiens* β-chain hemoglobin; *Hsa NGB*, *H. sapiens* neuroglobin; *Aac Ngb*, *A. aculeata* nerve hemoglobin; *Cla nHb*, *C. lacteus* nerve hemoglobin; *Lpe Hb1*, *L. pectinata* hemoglobin 1; *Ali Mb*, *Aplysia limacina* myoglobin; *Sso nHb*, *S. solidissima* nerve hemoglobin. Partial amino acid sequence of the *S. solidissima* nHb derived by Edman degradation of the tryptic peptides is *underlined*.

mal mode and a liquid nitrogen-cooled CCD detector. The excitation source was a Kr-ion laser (Spectra Physics 2020) at 413.1 nm. The protein solution was stirred at 6,000 rpm to avoid local heating. Five spectra (120-s recording time) were acquired and averaged after the removal of cosmic ray spikes by a program developed in-house. Laser powers of 2 and 17 milliwatts were used.

Sample Preparation—The CO form of the sample was prepared by adding an excess of sodium dithionite and subsequently passing the sample through a PD10 column (Amersham Biosciences) equilibrated with CO-flushed Tris-HCl buffer (5 mM, pH 8.5). The deoxyferrous form was obtained by equilibration under nitrogen and by adding an excess of sodium dithionite. The concentration of the protein samples used for optical and RR measurements was typically ~60 μM in Tris-HCl buffer (5 mM, pH 8.5).

Kinetic and Equilibrium Measurements of Ligand Binding to Native and Recombinant S. solidissima nHb—Oxygen affinity and cooperativity of recombinant nHb were measured in 0.1 M Tris buffer, 0.5 mM EDTA, at pH 7.5 and 20 °C using a thin-layer gas diffusion chamber as previously described (25). Briefly, 4-μl samples were allowed to equilibrate with various O_2/N_2 gas mixtures, while the absorbance at 428 nm was continuously monitored using a UV-VIS Cary 50 Probe spectrophotometer equipped with optic fibers. pH was measured in 100-μl subsamples using a BMS 2 MK 2 thermostated microelectrode (Radiometer). Values for O_2 affinity (P_{50}, O_2 tension at half-saturation) and cooperativity (n_{50}) were interpolated from the zero-intercept and the slope, respectively, of Hill plots, $\log[Y/(1-Y)]$ *versus* $\log PO_2$, where Y is the O_2 saturation.

Ligand recombination kinetics were measured by flash photolysis as previously described (31). Photolysis of the CO form was achieved with laser pulses at 532 nm (Quantel). The subsequent return to the CO bound form involves a competitive binding of the CO and the sixth (protein) ligand. Several detection wavelengths were used to better separate the different spectroscopic species. These kinetics allow the determination of the CO on-rate, and both the on and off rates for the protein ligand. In a similar fashion, a mixed atmosphere of CO and oxygen was used to obtain the oxygen binding rates.

Molecular Phylogenetic Analysis—Amino acid sequences of mollusc globins and the *S. solidissima* nHb were added manually to an established alignment of globin sequences (1, 32, 33). The selected sequences of mollusc Hbs and Mbs comprise *Anadara trapezia* (ark shell) HbIB (GenBank™ accession number P04251) and HbIIB (AtrHbIB, P14394); *Barbatia lima* (blood clam) HbA (BliHbA, S61520); *Barbatia virescens* (blood clam) HbI (BviHbI, AAB24577); *Lucina pectinata* HbI (LpeHbI, P41260), HbII (LpeHbII, P41261) and HbIII (LpeHbIII, P41262); *Scapharca broughtonii* HbI (SbrHbI, P02212); *Scapharca inaequivalvis* (ark clam) HbIIB (SinHbIIB, S09068); *Dolabela auricularia* (sea hare) Mb (DauMb, P09965); *Nassa mutabilis* (mutable nassa) Mb (NmuMb, P31331); *Busycon canaliculatum* (channeled whelk) Mb (BcaMb, P02214); *Cerithidae rhizophorarum* (water snail) Mb (CrhMb, P02215). The alignment further included the sequences: *Homo sapiens* NGB (HsaNGB, AJ245946), cytoglobin (HsaCYGB, AJ315162), Mb (HsaMB, M14603), and Hb α (HsaHBA, J00153), Hb β (HsaHBB, M36640), Hb δ (HsaHBD, AAH69307), Hb ϵ (HsaHBE, P02100); *Mus musculus* Ngb (MmuNgb, AJ245946), Cygb (MmuCygb, AJ315163) and Mb (MmuMb, P04247); *A. aculeata* nHb (Aac nHb, U46754); *Glycera dibranchiata* (bloodworm) Hb1 (GdiHb1, GGNW1B); *Ciona intestinalis* (sea squirt) Hbs 1 to 4 (CinHb1–4, AJ548500, AJ548501, AJ548502, AJ557135); *C. lacteus* (milky ribbon-worm) nHb (ClaHb, O76242); *Medicago sativa* (alfalfa) leghemoglobin (MsaLegHb, P09187); *Lupinus luteus* (alfalfa) leghemoglobin (LluLegHb, P02240); *Casuarina glauca* (swamp oak) Hb1 (CglHb1, P08054) and Hb2 (CglHb2, P23244); *Oryza sativa* (rice) Hb2 (OsaHb2, O04985).

For the reconstruction of phylogenetic trees, the program packages TREE-PUZZLE 5.0 (34), PHYLIP 3.6b (35), MEGA2 (36), and MrBayes 3.0 (37) were used. Bayesian phylogenetic analyses were performed with MrBayes 3.0 beta4, assuming the WAG substitution matrix model (38)

Downloaded from www.jbc.org at Marine Biological Laboratory on April 21, 2009

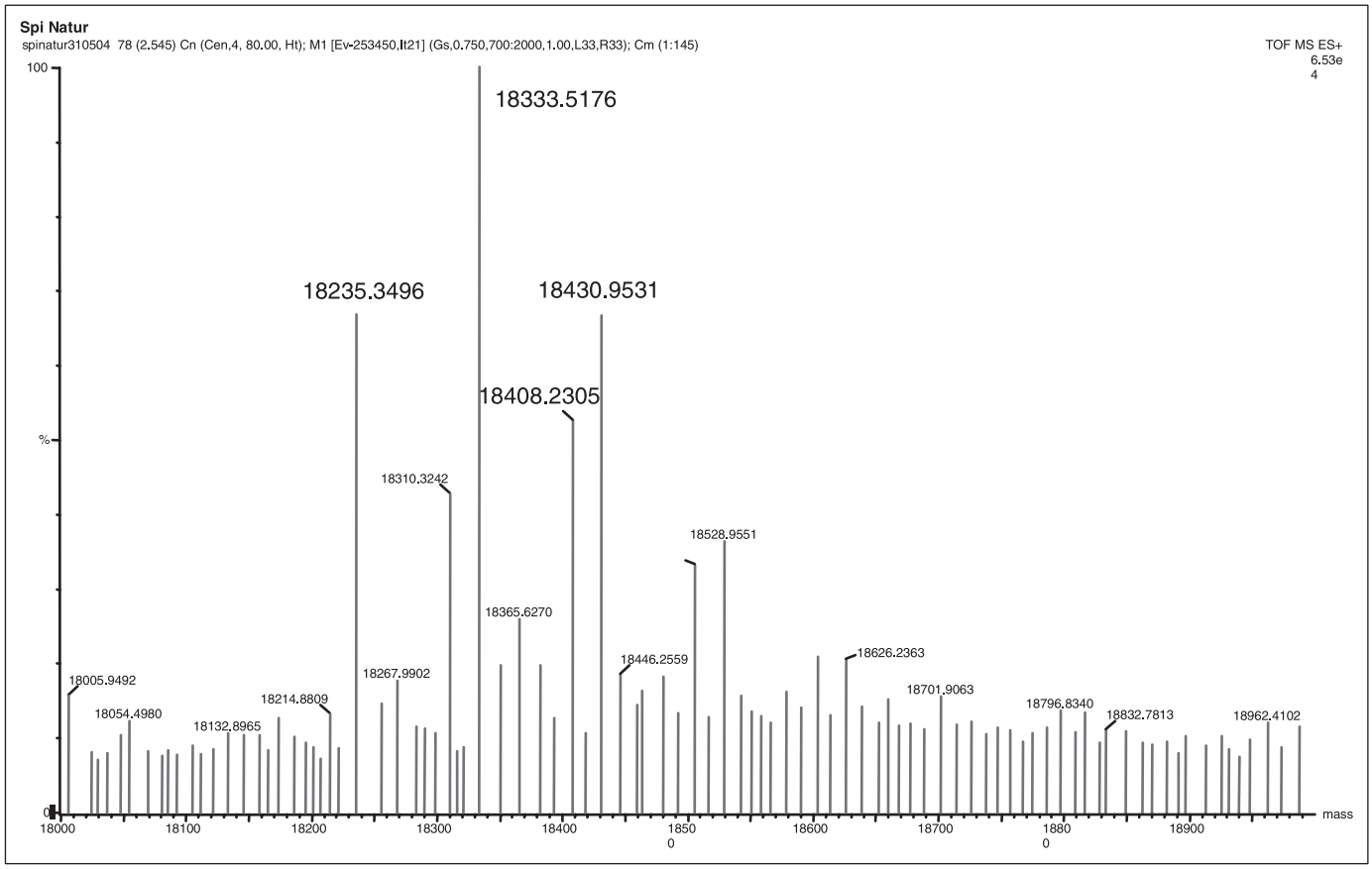

FIGURE 2. **Mass spectrum of native *S. solidissima* nHb.** Intensity of the peaks plotted against the molecular mass.

of sequence evolution with gamma distribution of rates. Metropolis-coupled Markov chain Monte Carlo sampling was performed with one cold and three heated chains that were run for 600,000 generations. Starting trees were random, trees were sampled every 10th generation, and three independent runs were performed. The posterior probabilities were estimated on the final 50,000 trees (burn-in, 10,000).

For neighbor-joining analyses (39), protein distances were calculated using the PAM substitution matrix (40). The programs NEIGHBOR from the PHYLIP package and MEGA version 2.1 were employed for tree reconstruction. In the case of applying the program NEIGHBOR, TREE-PUZZLE 5.2 was used for calculation of distance matrices. The reliability of the trees was tested by bootstrap analyses (41) with 1,000 replications.

RESULTS AND DISCUSSION

Primary Structure and Gene Organization—A part of the *S. solidissima* nHb primary structure was reconstructed from the sequence of relevant peptides generated by tryptic digestion of the purified protein (Fig. 1). The full sequence was completed by sequencing the corresponding cDNA of the nHb (GenBank™ accession number AM086629). Fig. 1 also shows the alignment of the *S. solidissima* nHb with related globin sequences. Key amino acid positions of the globin structure such as NA2, B6, B14, C2, CD1, E7, F8, and H8 are conserved (42). At the N terminus there is an extension of ~6 amino acid residues, the fourth one being a cysteine. A second cysteine is present at position E12. Otherwise there are no remarkable amino acid substitutions compared with other mollusc hemoglobins (see Fig. 1). Conceptual translation of the 162-amino acid-long sequence predicted a molecular mass of 18,191 Da, excluding the N-terminal methionine. However, mass spectrometry data on the intact native nerve globin showed a molecular mass of 18,235 Da, which confirms the absence of the N-terminal methionine and suggests an N-terminal mono-acetylation (+42 Da). This is not so unusual as N-terminal acetylation is one of the most common protein modifications in eukaryotes, occurring on ~85% of the different varieties of eukaryotic proteins but rarely on prokaryotic proteins (43, 44). We observed two additional molecular mass classes (18,333 and 18,430 Da) that differ from the native mono-acetylated protein by 98 and 196 Da, respectively (Fig. 2). These additional masses could agree with a binding of a mono- and a diphosphate to the nHb. Their physiological role, however, is unclear. The recombinant protein gave the single mass of 18,192 Da, with no additional acetylation. There was, however, an additional molecular mass class of 18,289 Da, suggesting again the presence of a phosphate. The binding of phosphate groups to both native and recombinant *S. solidissima* nHb was confirmed by ProQ Diamond phosphoprotein staining (data not shown).

Genomic DNA was extracted from *S. solidissima* foot and contractor muscle and pooled from multiple animals. The nHb gene was amplified by PCR and sequenced both directly and after cloning to resolve observed sequence heterogeneities. The obtained sequence (GenBank™ accession number AM086630) contained differences in the intronic regions probably representing allelic polymorphisms, whereas only two variations in the coding exons were observed. We noted 51 single nucleotide polymorphisms and 4 insertion/deletion polymorphisms in the intronic regions, varying in length from 1 to 284 bp. The coding region of the *S. solidissima* nHb gene is distributed on three exons, consisting of 116, 226, and 144 bp (measured from the ATG start codon and excluding the stop codon), validating the results from the cDNA. The two introns contain standard splice donor and acceptor

Downloaded from www.jbc.org at Marine Biological Laboratory on April 21, 2009

motifs, and they are located at positions B12.2 (*i.e.* between the second and third base of the 12th codon in helix B of the globin) and G7.0. The presence of the B12.2 and G7.0 intron positions is a conserved hallmark of vertebrate (and many invertebrate) globin genes. The *S. solidissima* nHb gene does not contain a third intron within the E helix region, which is characteristic for the Ngb gene lineage in vertebrates and urochordates (1, 33, 45).

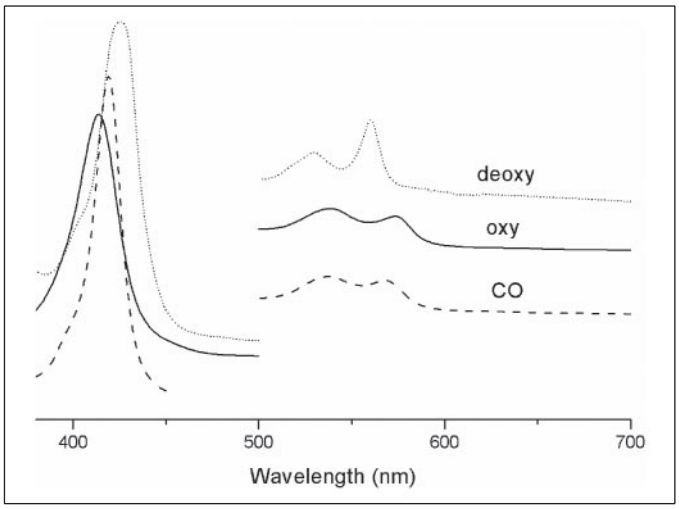

FIGURE 3. **Optical spectra of *S. solidissima* nHbO$_2$ (*solid line*), deoxy nHb (*dotted line*), and nHbCO (*dashed line*).**

Optical and RR Spectra—The optical spectrum of the ferrous oxy form of recombinant *S. solidissima* nHb (see Fig. 3) displays a Soret band at 414 nm. The α and β bands in the visible region are found at 537 and 573 nm, respectively, as reported earlier by Strittmatter and Burch (14). Similar values were observed for the oxy form of *Paramecium* Hb (46) and sperm whale Mb (47). For nHbCO, the Soret band is shifted to a slightly higher wavelength (420 nm), which is in agreement with the optical spectrum of the CO form of *Paramecium* Hb (46). The α and β bands of nHbCO are situated at 537 and 568 nm, again in good agreement with the CO form of *Paramecium* Hb (46). In the absorption spectrum of deoxyferrous *Spisula* nHb the Soret band appears at 426 nm. The α and β bands arise at 530 and 560 nm, respectively. These values were also found for non-symbiotic barley Hb (48), non-symbiotic rice Hb (49), Ngb (15), and cytoglobin (Cygb) (50). The values are typical for ferrous low spin heme complexes with a hexacoordination of the iron atom. The amino acid sequence of *S. solidissima* nHb indicates that the sixth ligand of the iron atom in the deoxy form is most likely E7His.

The RR spectra of nHbO$_2$, deoxyferrous nHb, and nHbCO are shown in Fig. 4. It is well established that the marker lines ν_4, ν_3, and ν_2 in the high frequency region of the RR spectrum are sensitive to the oxidation state, spin state, and coordination number of the iron at the center of the heme pocket. In the RR spectrum of nHbO$_2$ (see Fig. 4, *aA* and *bA*), ν_4, ν_3, and ν_2 are situated at 1373, 1507, and 1578 cm^{-1}, respectively, in agreement with earlier studies on heme proteins in the oxy form, *e.g.* the oxy complex of *Paramecium* Hb (46). Upon increase of the laser power to 17 milliwatts, a second spectral component appears. The ν_4 peak of

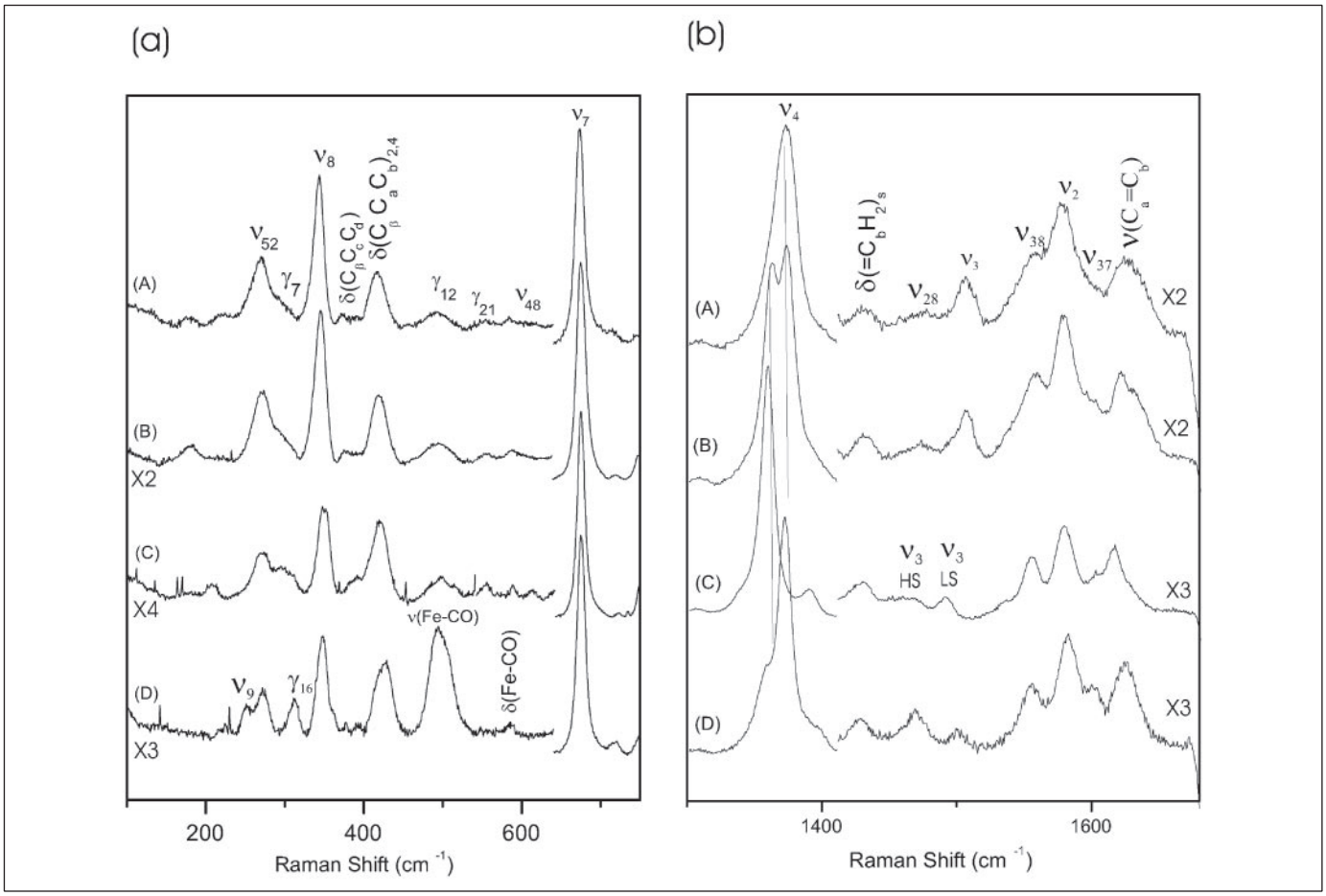

FIGURE 4. **Low frequency (*a*) and high frequency (*b*) resonance Raman spectra of *S. solidissima* nHbO$_2$ (laser power 2 milliwatts) (*A*), nHbO$_2$ (laser power 17 milliwatts) (*B*), deoxy nHb (laser power 17 milliwatts) (*C*), and nHbCO (laser power 2 milliwatts) (*D*).**

Downloaded from www.jbc.org at Marine Biological Laboratory on April 21, 2009

this new component is positioned at 1363 cm^{-1} (see Fig. 4, *aB* and *bB*), which agrees with the formation of the photoproduct. This is confirmed by the RR spectrum of ferrous deoxy nHb, obtained after reduction with sodium dithionite (see Fig. 4, *aC* and *bC*). ν_4, ν_3, and ν_2 are situated at 1360, 1491, and 1580 cm^{-1}, respectively, typical for a hexacoordinate low spin Fe^{II} heme form, confirming the absorption data (Fig. 3, *dotted lines*). Furthermore, a high spin (HS) component is present, as is indicated by the lines at 1470 (ν_3) and 1555 cm^{-1} (ν_2). Note that the intensity of the HS ν_3 marker line is lower than the intensity of the LS ν_3 marker line. This suggests that there is only a very small HS population present, as the intensity of ν_3 is very high for pentacoordinated species in comparison with hexacoordinated species. A small HS component has been found for other *bis*-histidine-coordinated globins (51).

In the spectrum of *S. solidissima* nHbCO ν_4, ν_3, and ν_2 are located at 1373, 1500, and 1583 cm^{-1}, respectively, characteristic for a hexacoordinated low spin complex. Again, the lines at 1460 (ν_4), 1469 (ν_3), and 1556 cm^{-1} (ν_2) indicate that there is a small population of an HS ferrous complex present, which agrees with a small fraction of photodissociation taking place. Two CO coordination configurations can be distinguished, one with the Fe-CO stretching mode at 494 cm^{-1} (75%) and one with this mode at 513 cm^{-1} (25%) (see supplemental information). The first configuration (494 cm^{-1}) was observed previously, *e.g.* in sperm whale Mb (491 cm^{-1}) (52). In Mb, this conformer becomes dominant at low pH values, when E7His swings out of the heme pocket. It is ascribed to an open conformation of the heme pocket, with a weak interaction between CO and the surrounding amino acids. The second conformer (513 cm^{-1}) was also observed in Mb (508 cm^{-1}) (52) and Cygb (510 cm^{-1}) (50) and was assigned to a conformation in which the heme pocket is closed, due to the stabilization of CO by E7His. Note that no Fe-CO stretching modes at higher frequencies are observed, in contrast to several other heme proteins capable of a *bis*-histidine coordination of the heme iron, such as Ngb (523 cm^{-1}) (51), Cygb (518 cm^{-1}) (50), or *Barley* Hb (534 cm^{-1}) (53). Higher Fe-CO stretching frequencies correspond to a stronger stabilization of CO, *e.g.* due to interaction with several surrounding amino acid residues. The line at 586 cm^{-1} can be attributed to the Fe-C-O bending mode. Note that the bending mode is weak, which is typical for an open conformation of the heme pocket. It was previously shown that the conformation of the heme pocket can differ significantly for O_2 and CO binding (46). Also, it has been shown that when the distal His is able to interact with the bound oxygen closed conformation of the heme pocket autoxidation is greatly enhanced, as the ferrous O_2 acquires more ferric O_2^- (superoxide) character (25).

Kinetic and Equilibrium Measurements of Ligand Binding to Native and Recombinant S. solidissima nHb—Fig. 5 shows the oxygen equilibrium curve for recombinant *S. solidissima* nHb at 20 °C, pH 7.5 and the data expressed as a Hill plot (*inset*). Under these conditions, the oxygen affinity is high, with a P_{50} value of ~0.6 torr, and oxygen is bound in a non-cooperative manner as indicated by a slope of ~1 in the Hill plot. The P_{50} and *n* values found in our study on the recombinant protein are significantly lower than those reported from *in situ* measurements on intact nerves at high protein concentrations, where a P_{50} of 2.3 torr and an *n* value of 2.1 were found (28). The difference in P_{50} and *n* values may arise because our measurements were carried out *in vitro* on a recombinant protein, whereas the previous data refer to the native protein in its natural environment, indicating *in vivo* aggregation at high concentration and/or the existence of *in vivo* allosteric effectors that lower oxygen affinity. Acetylation of the native protein, but not the recombinant one, may also contribute to the observed functional differences. Indeed Lacan *et al.* (54) showed that a new α-chain variant, Hb Lyon-Byron, is characterized by the replacement of the N-terminal valine by an alanine that is N-terminal acetylated. This resulted in a decreased oxygen affinity.

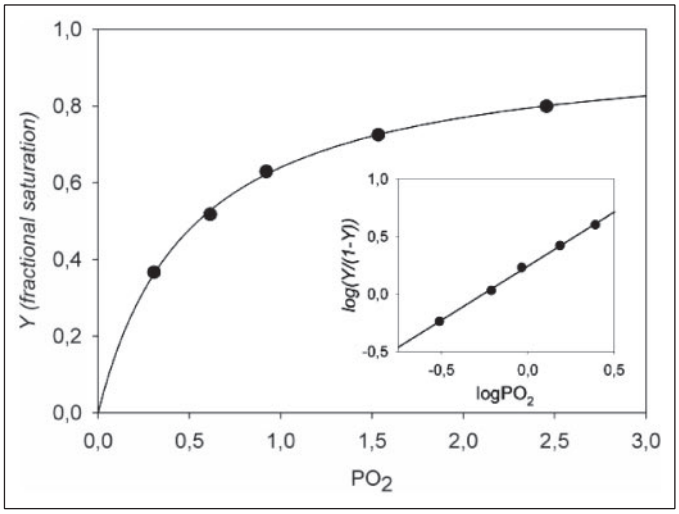

FIGURE 5. **Oxygen equilibrium curve and Hill plot (*inset*) of *S. solidissima* nHb measured at 20 °C in 0.1 M Tris buffer, pH 7.5.** The protein concentration was 0.11 mM heme. PO_2 is expressed in torr. Absence of cooperativity of oxygen binding can be inferred from the unitary slope of the Hill plot.

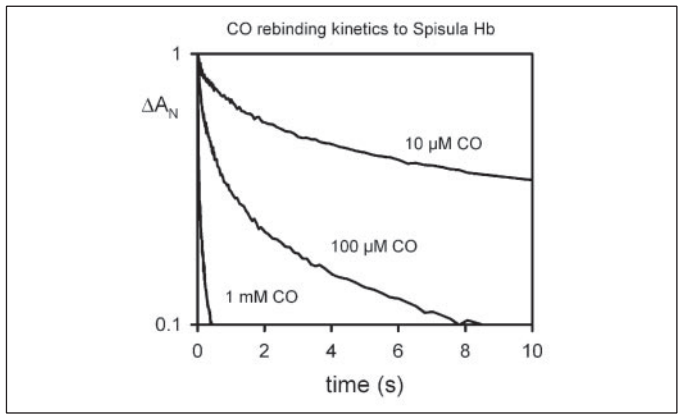

FIGURE 6. **CO rebinding kinetics of *S. solidissima* nHb.** After photodissociation, there is competitive binding of CO and the protein (E7 His) ligand. At high CO levels, one observes mainly a single phase of CO recombination. At lower CO levels, His binding becomes competitive and the second phase is more prominent. The rate of the second phase corresponds to the rate of replacement of His by CO.

TABLE 1
Ligand binding kinetics
The affinity P_{50} was calculated using the formula $P_{50} = (K_{penta}O_2)^*(1 + KHis)$. The O_2 solubility coefficient was taken equal to 1.82 μM/torr.

	$k_{on}CO$	$k_{on}O_2$	$k_{off}O_2$	$K_{penta}O_2$	$k_{on}His$	$k_{off}His$	*K*His	P_{50} calculated	P_{50} measured
	M/s × 10^7	*M/s* × 10^7	*s*	*n*M	*s*	*s*		*torr*	
S. solidissima nHb	7.5	13	30	230	14000	1000	14	1.9	0.6
M. musculus Ngb	5.5	20	0.4	2	1000	0.5	2000	2.2	
Horse Mb	0.5	1.6	24	1500				0.8	

Downloaded from www.jbc.org at Marine Biological Laboratory on April 21, 2009

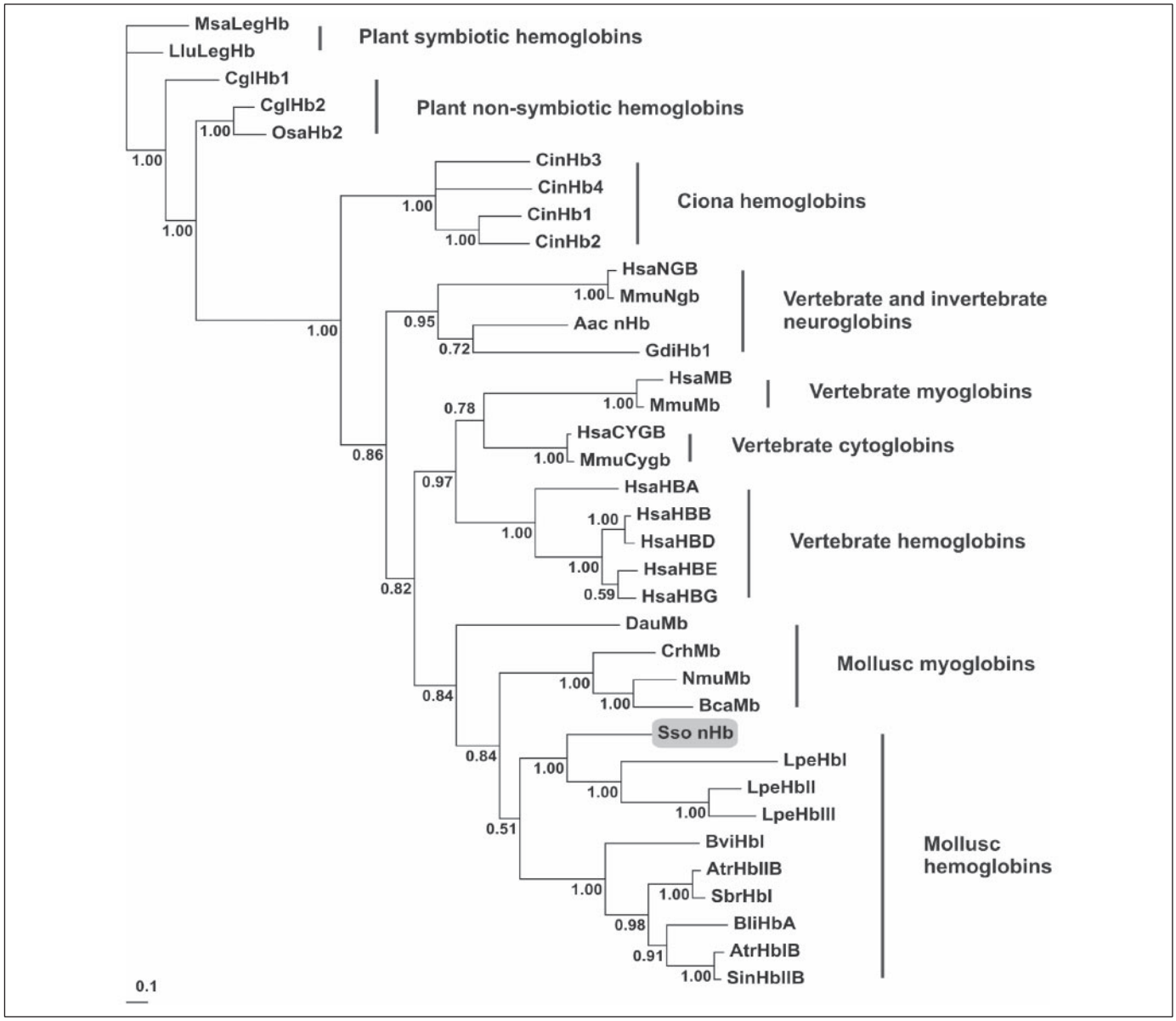

FIGURE 7. **Bayesian phylogenetic tree of vertebrate, invertebrate, and plant globins based on amino acid sequence data.** The *S. solidissima* nHb (*shaded*) clearly groups with other mollusc hemoglobins, but not with vertebrate Ngbs or the Ngb-related nerve globin from the annelid *A. aculeata*. The posterior probabilities of clade support are shown at the branches. Three-letter species designations are specified under "Materials and Methods."

Flash photolysis experiments show two kinetic components for monomers of recombinant *S. solidissima* nHb. This type of kinetics is the result of competitive binding of two ligands, as previously observed for other hexacoordinate globins such as vertebrate Ngb or Cygb (15, 23). In the case of the *S. solidissima* nHb the separation of the kinetic phases is less distinct, as the coefficient for His binding is only ~10 as compared with >1,000 for certain forms of Ngb.

The ligand binding rates for CO and oxygen are both quite high (Table 1, Fig. 6), with oxygen having the higher rate, as generally observed for heme proteins. The value for oxygen association is among the highest observed, approaching the diffusion limit for the bimolecular globin ligand reaction.

The histidine association rate is an order of magnitude higher than that observed for other hexacoordinated globins, although there are relatively few values available for comparison. Binding of the histidine requires only 100 μs compared with 1 ms for Ngb; Cygb is relatively slow, requiring ~10 ms (15, 23). The His dissociation occurs in ~1 ms, resulting in a binding coefficient of ~10 for the hexacoordination of *S. solidissima* nHb. Because of these elevated rates for His binding, there is significant overlap with the CO binding phase and the two kinetic phases are less distinct than for the case of Ngb. In the case of human Ngb, there is an influence of an internal disulfide bond on the His kinetics (55), which can be probed by addition of dithiothreitol to break the bond. There was no effect of the dithiothreitol on the *S. solidissima* nHb binding kinetics. This was expected, as the 2 cysteine residues present (in positions NA4 and E12) are unlikely to form a disulfide bond.

The O_2 affinity obtained from the kinetic data (P_{50}, 1.9 torr) is in fairly good agreement with the value determined by equilibrium measurements (P_{50}, 0.6 torr). Small differences can be because of the difference in experimental approaches. From the kinetics, one can separate the intrinsic oxygen binding parameters from the contribution of the His affinity (Table 1).

We can conclude from the above described experiments (spectra and ligand binding properties) that *S. solidissima* nHb can be classified as

Downloaded from www.jbc.org at Marine Biological Laboratory on April 21, 2009

normal intracellular hemoglobin having a "myoglobin-like" function. The major structural characteristic is the hexacoordinated nature of the iron atom. The structural differences between penta- and hexacoordinated hemoglobins might be, however, very small. Indeed, vertebrate Hb and Mb, normally pentacoordinated, shift toward hexacoordination (hemichrome) near their denaturation point because of a reorganization of their heme pocket (56–58). Application of high pressure (0.1–700 MPa) to penta- or partially hexacoordinated Hbs can also increase the percentage of hexacoordination. This shift results in a difference of ligand binding characteristics (59).

Phylogenetic Analyses—The amino acid sequence of the *S. solidissima* nHb has an average identity of only 16–20% and a similarity (calculated using the PAM250 matrix) of 30% to vertebrate Ngbs and Cygbs. In contrast, it displays 23–30% amino acid identity and 39–50% similarity to other mollusc Hbs and Mbs. The amino acid sequence of the nHb was added to an alignment of selected vertebrate and invertebrate globin sequences (1, 32, 33), including representative mollusc globins. Phylogenetic trees were calculated using the Bayesian approach (Fig. 7) and the neighbor-joining distance method (not shown). Trees were rooted considering plant leghemoglobin as out-group. Regardless of the reconstruction method used, the *S. solidissima* nHb formed a common clade with the mollusc Hbs and consistently grouped with the gill Hbs of the bivalve mollusc *L. pectinata*. These cytoplasmic Hbs are specialized to supply either O_2 (Hb2 and 3) or sulfide (Hb1) for metabolism, probably playing a role in the symbiosis of these molluscs and chemoautotrophic bacteria (5).

In contrast to the *S. solidissima* nHb, the nHb of the annelid *A. aculeata* (6) grouped with vertebrate Ngb sequences as described before (1). The highly derived and phylogenetically less informative nHb sequence from the nemertean worm *C. lacteus* (7) tended to group at various positions basal to the Ngb gene lineage and was therefore excluded from the final tree reconstruction (data not shown). This behavior is most likely based on its structural shortening of the globin rather than on its phylogenetic position (7).

Implications for Vertebrate and Invertebrate Nerve Globin Function—The nervous system of both vertebrates and invertebrates requires huge amounts of metabolic energy and thus oxygen. It is therefore not surprising that neurons are highly vulnerable to any shortage in oxygen supply as it occurs under pathological (*e.g.* ischemia) or natural hypoxic conditions (60). There is no doubt that respiratory proteins that either enhance oxygen flow under normoxic conditions or store oxygen for short-term hypoxic states should be evolutionarily advantageous for the survival of neurons and thus are frequently found in the nervous systems of various invertebrate taxa (4). Strongly expressed, glial nHbs like the one in the bivalve mollusc *S. solidissima* are present in those species that encounter substantial hypoxia in their natural habitats (4, 5). Physiological experiments have convincingly demonstrated that glial nHbs enable these bivalves to maintain neuronal function while burrowing in O_2-poor sediments (9, 29). Our biochemical characterization of the *S. solidissima* nHb is generally in line with the proposed O_2 supply function, *e.g.* by confirming the Mb-like O_2 affinity of this respiratory protein. There are, however, additional unusual features of the *S. solidissima* nHb (phosphate binding, iron hexacoordination, etc.), the roles of which in the nHb respiratory function are not yet clear.

Originally, it had been proposed that invertebrate nHbs are phylogenetically orthologous to vertebrate Ngbs (1). This notion was based on the finding that in phylogenetic analyses the nHb of the annelid *A. aculeata* consistently groups with human and mouse Ngb (Ref. 1 and this report; Fig. 7). However, here we have shown that the nHb of the bivalve mollusc *S. solidissima* does not belong to the "Ngb plus *A. aculeata* nHb" clade but groups with the other mollusc Hbs and Mbs. This finding demonstrates that a classical Hb or Mb has been recruited during evolution to fulfill the task of providing O_2 to the nerve cells of *S. solidissima*. Invertebrate nHbs are therefore of polyphyletic origin. Consequently, mollusc glial nHbs will probably have only modest relevance as a model for studying the function of Ngb in the nervous system of vertebrates (2). We note, however, that less prominently expressed nHbs, coupled to a neuronal expression site, have been reported, *e.g.* for air-breathing gastropod molluscs (11), which like most vertebrates do not encounter substantial environmental hypoxia. This feature of a neuron-specific, low-expressed nHb is a clear parallel to vertebrate Ngbs. It will therefore be interesting to investigate the phylogenetic affiliation, biochemical features, and cellular function of invertebrate "neuronal" nHbs in comparison with the invertebrate glial nHbs and neuronal vertebrate Ngb.

Independent Origin of Hb Hexacoordination—From a biochemical perspective, it is noteworthy that the *S. solidissima* nHb represents the first true respiratory Hb to be found in an iron-hexacoordinated form, resembling in this respect the vertebrate Ngb proteins (15, 61). This confirms an earlier suggestion that a *bis*-His-Fe hexacoordinate heme structure has arisen independently in distinct globin lineages (45). The *S. solidissima* nHb will be instrumental as a model in studying the evolutionary determinants of this protein feature.

Acknowledgment—Thierry Backeljau is acknowledged for the help with dissections of the Spisula nerve strains.

REFERENCES

1. Burmester, T., Weich, B., Reinhardt, S., and Hankeln, T. (2000) *Nature* **407,** 520–523
2. Hankeln, T., Ebner, B., Fuchs, C., Gerlach, F., Haberkamp, M., Laufs, T. L., Roesner, A., Schmidt, M., Weich, B., Wystub, S., Saaler-Reinhardt, S., Reuss, S., Bolognesi, M., de Sanctis, D., Marden, M. C., Kiger, L., Moens, L., Dewilde, S., Nevo, E., Avivi, A., Weber, R. E., Fago, A., and Burmester, T. (2005) *J. Inorg. Biochem.* **99,** 110–119
3. Lankester E. R. (1872) *Proc. R. Soc. Lond. B Biol. Sci.* **21,** 70–81
4. Wittenberg, J. B. (1992) in *Advances in Comparative and Environmental Physiology* (Mangum, C. P., ed) pp. 59–85, Springer-Verlag Berlin, Heidelberg
5. Weber, R. E., and Vinogradov, S. N. (2001) *Physiol. Rev.* **81,** 569–628
6. Dewilde, S., Blaxter, M., Van Hauwaert, M. L., Vanfleteren, J., Esmans, E. L., Marden, M., Griffon, N., and Moens, L. (1996) *J. Biol. Chem.* **271,** 19865–19870
7. Vandergon, T. L., Riggs, C. K., Gorr, T. A., Colacino, J. M., and Riggs, A. F. (1998) *J. Biol. Chem.* 16998–17011
8. Chalazonitis, N., Gola, M., and Arvanitaki, A. (1966) *C. R. Seances Soc. Biol. Fil.* **160,** 1020–1023
9. Kraus, D. W., and Colacino, J. M. (1986) *Science* **232,** 90–92
10. Kraus, D. W., Doeller, J. E., and Smith, P. R. (1988) *Biol. Bull.* **174,** 54–66
11. Schindelmeiser, I., Kuhlmann, D., and Nolte, A. (1979) *Comp. Biochem. Physiol. B* **64B,** 149–154
12. Wittenberg, B. A., Briehl, R. W., and Wittenberg, J. B. (1965) *Biochem. J.* **96,** 363–371
13. Arvanitaki, A., and Chalazonitis, N. (1960) *Bull. Inst. Oceanogr. Monaco* **1164,** 1–83
14. Strittmatter, P., and Burch, H. B. (1963) *Biochim. Biophys. Acta* **78,** 562–563
15. Dewilde, S., Kiger, L., Burmester, T., Hankeln, T., Baudin-Creuza, V., Aerts, T., Marden, M. C., Caubergs, R., and Moens, L. (2001) *J. Biol. Chem.* **276,** 38949–38955
16. Kiger, L., Uzan, J., Dewilde, S., Burmester, T., Hankeln, T., Moens, L., Hamdane, D., Baudin-Creuza, V., and Marden, M. (2004) *IUBMB Life* **56,** 709–719
17. Burmester, T., Haberkamp, M., Mitz, S., Roesner, A., Schmidt, M., Ebner, B., Gerlach, F., Fuchs, C., and Hankeln, T. (2004) *IUBMB Life* **56,** 703–707
18. Reuss, S., Saaler-Reinhardt, S., Weich, B., Wystub, S., Reuss, M. H., Burmester, T., and Hankeln, T. (2002) *Neuroscience* **115,** 645–656
19. Geuens, E., Brouns, I., Flamez, D., Dewilde, S., Timmermans, J. P., and Moens, L. (2003) *J. Biol. Chem.* **278,** 30417–30420
20. Schmidt, M., Giessl, A., Laufs, T., Hankeln, T., Wolfrum, U., and Burmester, T. (2003) *J. Biol. Chem.* **278,** 1932–1935
21. Wystub, S., Laufs, T., Schmidt, M., Burmester, T., Maas, U., Saaler-Reinhardt, S., Hankeln, T., and Reuss, S. (2003) *Neurosci. Lett.* **346,** 114–116
22. Laufs, T. L., Wystub, S., Reuss, S., Burmester, T., Saaler-Reinhardt, S., and Hankeln, T. (2004) *Neurosci. Lett.* **362,** 83–86
23. Pesce, A., Bolognesi, M., Bocedi, A., Ascenzi, P., Dewilde, S., Moens, L., Hankeln, T., and Burmester, T. (2002) *EMBO Rep.* **3,** 1146–1151

Downloaded from www.jbc.org at Marine Biological Laboratory on April 21, 2009

24. Moens, L., and Dewilde, S. (2000) *Nature* **407,** 461–462
25. Fago, A., Hundahl, C., Dewilde, S., Gilany, K., Moens, L., and Weber, R. E. (2004) *J. Biol. Chem.* **279,** 44417–44426
26. Sun, Y., Jin, K., Mao, X. O., Zhu, Y., and Greenberg, D. A. (2001) *Proc. Natl. Acad. Sci. U. S. A.* **98,** 15306–15311
27. Sun, Y., Jin, K., Peel, A., Mao, X. O., Xie, L., and Greenberg, D. A. (2003) *Proc. Natl. Acad. Sci. U. S. A.* **100,** 3497–3500
28. Kraus, D. W., and Doeller, J. E. (1988) *Biol. Bull.* **174,** 346–354
29. Doeller, J. E., and Kraus, D. W. (1988) *Biol. Bull.* **174,** 67–76
30. Schmidt, E. R., Vistorin, G., and Keyl, H. G. (1980) *Chromosoma* **76,** 35–45
31. Uzan, J., Dewilde, S., Burmester, T., Hankeln, T., Moens, L., Hamdane, D., Marden, M. C., and Kiger, L. (2004) *Biophys. J.* **87,** 1196–1204
32. Burmester, T., Ebner, B., Weich, B., and Hankeln, T. (2002) *Mol. Biol. Evol.* **19,** 416–421
33. Ebner, B., Burmester, T., and Hankeln, T. (2003) *Mol. Biol. Evol.* **20,** 1521–1525
34. Strimmer, K., and von Haeseler, A. (1996) *Mol. Biol. Evol.* **13,** 964–969
35. Felsenstein, J. (2004) PHYLIP (Phylogeny Inference Package) Version 3.6b, Department of Genetics, University of Washington, Seattle
36. Kumar, S., Tamura, K., Jakobsen, I. B., and Nei, M. (2001) *Bioinformatics* **17,** 1244–1245
37. Huelsenbeck, J. P., and Ronquist, F. (2001) *Bioinformatics* **17,** 754–755
38. Whelan, S., and Goldman, N. (2001) *Mol. Biol. Evol.* **18,** 691–699
39. Saitou, N., and Nei, M. (1987) *Mol. Biol. Evol.* **4,** 406–425
40. Dayhoff, M. O., Schwartz, R. M., and Orcutt, B. C. (1978) in *Atlas of Protein Sequence and Structure* (Dayhoff, M. O., ed) pp. 345–352, National Biomedical Research Foundation, Washington, D. C.
41. Felsenstein, J. (1985) *Evolution* **39,** 783–791
42. Bashford, D., Chothia, C., and Lesk, A. M. (1987) *J. Mol. Biol.* **196,** 199–216
43. Boissel, J. P., Kasper, T. J., Shah, S. C., Malone, J. I., and Bunn, H. F. (1985) *Proc. Natl. Acad. Sci. U. S. A.* **82,** 8448–8452
44. Polevoda, B., and Sherman, F. (2000) *J. Biol. Chem.* **275,** 36479–36482
45. Roesner, A., Fuchs, C., Hankeln, T., and Burmester, T. (2005) *Mol. Biol. Evol.* **22,** 12–20
46. Das, T. K., Weber, R. E., Dewilde, S., Wittenberg, J. B., Wittenberg, B. A., Yamauchi, K., Van Hauwaert, M. L., Moens, L., and Rousseau, D. L. (2000) *Biochemistry* **39,** 14330–14340
47. Antonini, E., and Brunori, M. (1971) *Hemoglobin and Myoglobin in Their Reaction with Ligands*, North Holland Publishing, Amsterdam
48. Duff, S. M., Wittenberg, J. B., and Hill, R. D. (1997) *J. Biol. Chem.* **272,** 16746–16752
49. Arrendondo-Peter, R., Hargrove, M. S., Sarath, G., Moran, J. F., Lohrman, J., Olson, J. S., and Klucas, R. V. (1997) *Plant Physiol.* **115,** 1259–1266
50. Sawai, H., Kawada, N., Yoshizato, K., Nakajima, H., Aono, S., and Shiro, Y. (2003) *Biochemistry* **42,** 5133–5142
51. Couture, M., Burmester, T., Hankeln, T., and Rousseau, D. L. (2001) *J. Biol. Chem.* **276,** 36377–36382
52. Sage, J. T., Morikis, D., and Champion, P. M. (1991) *Biochemistry* **30,** 1227–1237
53. Das, T. K., Lee, H. C., Duff, S. M., Hill, R. D., Peisach, J., Rousseau, D. L., Wittenberg, B. A., and Wittenberg, J. B. (1999) *J. Biol. Chem.* **274,** 4207–4212
54. Lacan, P., Souillet, G., Aubry, M., Prome, D., Richelme-David, S., Kister, J., Wajcman, H., and Francina, A. (2002) *Am. J. Hematol.* **69,** 214–218
55. Hamdane, D., Kiger, L., Dewilde, S., Green, B. N., Pesce, A., Uzan, J., Burmester, T., Hankeln, T., Bolognesi, M., Moens, L., and Marden, M. C. (2004) *Micron* **35,** 59–62
56. Keilin, J. (1949) *Biochem. J.* **45,** 440–448
57. Morishima, I., Ogawa, S., and Yamada, H. (1980) *Biochemistry* **19,** 1569–1575
58. Alden, R. G., Satterlee, J. D., Mintorovitch, J., Constantinidis, I., Ondrias, M. R., and Swanson, B. I. (1989) *J. Biol. Chem.* **264,** 1933–1940
59. Hamdane, D., Kiger, L., Hui Bon, H. G., Dewilde, S., Uzan, J., Burmester, T., Hankeln, T., Moens, L., and Marden, M. C. (2005) *J. Biol. Chem.* **280,** 36809–36814
60. Lee, J. M., Grabb, M. C., Zipfel, G. J., and Choi, D. W. (2000) *J. Clin. Investig.* **106,** 723–731
61. Pesce, A., Dewilde, S., Nardini, M., Moens, L., Ascenzi, P., Hankeln, T., Burmester, T., and Bolognesi, M. (2003) *Structure* **11,** 1087–1095

Downloaded from www.jbc.org at Marine Biological Laboratory on April 21, 2009